


Surface-based morphometry reveals caudate subnuclear structural damage in patients with premotor Huntington disease

Hosung Kim¹  · Ji-hoon Kim^{1,2} · Katherine L. Possin³ · Joseph Winer³ · Michael D. Geschwind³ · Duan Xu¹ · Christopher P. Hess^{1,3}

Published online: 11 October 2016
© Springer Science+Business Media New York 2016

Abstract In patients with premotor Huntington’s disease (pmHD), literature has reported decreases in caudate volume. However, the regional vulnerability of the caudate nucleus to pmHD remains to be clarified. We aimed to determine whether regional structural damage of the caudate nucleus was present in pmHD and was correlated with clinical profile using a surface-based morphometric technique applied to T1-weighted MRI. The study cohort consisted of 14 volunteers with genetically confirmed pmHD (6 males; 41.8 ± 13.2 years) and 11 age- and sex-matched controls (5 males; 46.2 ± 11.9 years, $p > 0.3$). On 3-T T1-weighted images, bilateral caudate volumes were manually delineated. The resulting labels were converted to a surface, triangulated with 1002 points equally distributed across subjects using SPHARM-PDM. Displacement vectors were then computed between each individual and a template surface representing the whole cohort. Computing point-wise Jacobian determinants (JD) from these vectors quantified local volumes. We found decreases in bilateral global caudate volumes in the pmHD group compared to controls ($t = 3.4$; $p = 0.002$). Point-wise analysis of local volumes mapped caudate atrophy in pmHD primarily onto medial surface ($t > 2.7$; FDR < 0.05), with most pronounced changes in anteromedial subdivision.

In a combined group of patients and controls, volume within the area presenting significant group difference was positively correlated with scores of executive function ($r = 0.7$; $p < 0.001$) and working memory ($r = 0.6$; $p = 0.002$). In patients, the caudate atrophy was associated with increase in disease burden ($r = 0.7$; $p = 0.005$). Caudate subnuclear atrophy measured using our surface-based morphometric technique is evident in pmHD, correlates with clinical variables, and may provide a more sensitive biomarker than global volumes.

Keywords Huntington disease · Surface-based morphometry · Caudate nucleus · MRI

Introduction

Huntington’s disease (HD) is an autosomal dominant neurodegenerative disorder caused by abnormal trinucleotide repeat within the *Huntingtin* gene, ultimately causing widespread cellular disruption across the brain (Dogan et al. 2013; Gusella et al. 1996). There is considerable variability in age of onset, symptom severity, and rate of progression across affected individuals. Prior to the diagnosis of manifest disease, which rests upon the clinical appearance of motor symptoms, there exist subtle cognitive and psychiatric symptoms (Duff, Paulsen, et al., 2007; Paulsen et al., 2008) and structural abnormalities of the brain (Cheng et al. 2011; Weir et al. 2011). Reliable biomarkers of subclinical disease progression are necessary to enable clinical trials of putative neuroprotective agents during a long potential therapeutic window (Vonsattel 2008; Weir et al. 2011; Finkbeiner 2010; Weir et al. 2011). Imaging of brain structures and subsequent morphometric analyses of early disease targets may provide a sensitive and

H. Kim and J. Kim contributed equally to the manuscript in this study.

✉ Hosung Kim
hosung.kim@ucsf.edu

¹ Department of Radiology and Biomedical Imaging, University of California San Francisco, San Francisco, CA, USA

² Department of Radiology, Seoul National University Hospital, Seoul, South Korea

³ Department of Neurology, University of California San Francisco, San Francisco, CA, USA

objective marker for monitoring progression in premotor Huntington's disease (pmHD).

Measures of caudate volume are a compelling choice for use as a marker of pmHD. The earliest neuropathologic changes, the loss of medium-sized spiny neurons, are seen within this structure. These have been documented more than a decade before diagnosis, and decrements progress reliably as diagnosis approaches (Aylward et al. 1996; Aylward et al. 2012; Dominguez et al. 2015; Paulsen et al. 2008). Further, caudate atrophy in pmHD is linked to declines in executive functions (Holl et al. 2013; You et al. 2014), which predict poor quality of life (Read et al. 2013).

The caudate nucleus is not a uniform structure (Kim et al. 2013a; Nakano 2000; Parent and Hazrati 1995; Postuma and Dagher 2006; Selemon and Goldman-Rakic 1988); rather, it consists of several distinctive functional zones: associative striatum (head of caudate), sensorimotor striatum (dorsolateral rim of the caudate), and the limbic striatum (ventral caudate). Analysis of the caudate in autopsy studies (Roos et al. 1985; Vonsattel et al. 1985a) suggests that volumetric changes are not uniform across these subregions. We thus hypothesized that atrophy would vary regionally across the volume of the caudate in pmHD, and that regionally atrophy would be related to measurements of executive functional deficit. To our knowledge, this has been investigated in two prior studies: one of which found no changes (van den Bogaard et al. 2011), and the other showed multiple sites of atrophy only in a subgroup with high genetic burden scores (Younes et al. 2014). Lack of sensitivity in these studies may have been due to the use of automated segmentation methods that were based on a single average template from the healthy population, which may be inaccurate for the segmentation of patient cases in which the striatum deviates from its normal shape.

To overcome the limitations of volumetric analysis based on a normal template, vertex (point)-wise morphometry based on a surface extracted from the manual segmentation has been suggested as a surrogate to manual subfield volumetry that can only be done with identification of the molecular layers, which is possibly visualized using ultra high-field (4–7 Tesla) and high-resolution MRI. These surface-based approaches have successfully detected hippocampal subfield abnormality in various brain disorders (Joo et al. 2014; Kim et al. 2013b). Herein, we aimed to determine whether regional structural damage of the caudate nucleus was present in premotor HD using a surface-based morphometry applied to T1-weighted MRI. To investigate progression of structural changes, we correlated the regional structural changes with scores of genetic disease burden and executive dysfunction in pmHD.

Materials and methods

Subjects

We studied 14 volunteers with genetically confirmed pmHD (6 males; 41.8 ± 13.2 years) and 11 age- and sex-matched controls (5 males; 46.2 ± 11.9 years, $p > 0.3$) who were recruited from a registry maintained by the UCSF Memory and Aging Center clinic or via their participation in other research projects at our institution between August 2011 and August 2013. Participants in the pmHD group tested positive for the HD mutation and had at least 40 CAG repeats. Neurologists with expertise in HD used the Unified Huntington's Disease Rating Scale (UHDRS) to determine the total motor score, between 0 and 124, and the diagnostic confidence level, between 0 (healthy, no abnormalities) and 4 (motor abnormalities consistent with HD, $\geq 99\%$ confidence), for each subject. The UCSF Committee on Human Research provided institutional review board approval for this Health Insurance Portability and Accountability Act-compliant prospective study, and written consent was obtained from all subjects.

Disease burden

CAG-Age-Product Scaled (CAPs), an index developed in the PREDICT-HD study to approximate the time to HD diagnosis by using the age at motor onset and the number of CAG repeats, was calculated for each subject with pmHD as $CAPs \times Age \times (CAG \times 33.66)/432.3326$ (Paulsen et al. 2006; Paulsen et al. 2008; Zhang et al. 2011). CAPs is classified as low ($0 < CAPs < 0.67$), medium ($0.67 < CAPs < 0.85$), or high ($CAPs > 0.85$), reflecting higher cumulative disease burden and closer proximity to diagnosis. According to previously established norms, CAPs of less than, equal to, or greater than 1 indicates a 5-year diagnosis probability of less than, equal to, or greater than 50 %, respectively.

Cognitive assessments

Executive function and working memory are especially vulnerable to early brain changes in pmHD (Duff et al. 2010; Hart et al. 2011; Stout et al. 2011). We assessed cognitive function in these domains by using the National Institutes of Health (NIH) EXAMINER (Kramer et al. 2014) Executive Composite and Working Memory Score. The Executive Composite is a global measure of executive function that includes measures of working memory, cognitive control, and fluency. The Working Memory Score includes measures of spatial and verbal working memory, which also contribute to the Executive Composite. Both measures are sensitive to cognitive changes and disease burden in pmHD (You et al. 2013).

MRI acquisition and image preprocessing

Subjects were scanned on 3 T MR imaging scanners (GE Healthcare, Milwaukee, Wisconsin) with 8 channel head coils. Volumetric T1-weighted imaging was performed using the following parameters: TR/TE = 7/2 ms, flip angle = 15°, FOV = 23 cm, matrix = 256 × 192, yielding the image resolution of 0.9 × 0.9 × 1 mm³. A subspecialty certified neuroradiologist (C.P.H.) reviewed all images to assess for subjective striatal atrophy was present with pmHD compared with controls.

Each image underwent automated correction for intensity non-uniformity (Sled et al. 1998) and was then spatially normalized using linear registration to the MNI-ICBM 152 non-linear template created using an unbiased framework for the construction of nonlinear average templates (Fonov et al. 2011).

Segmentation of the caudate nucleus

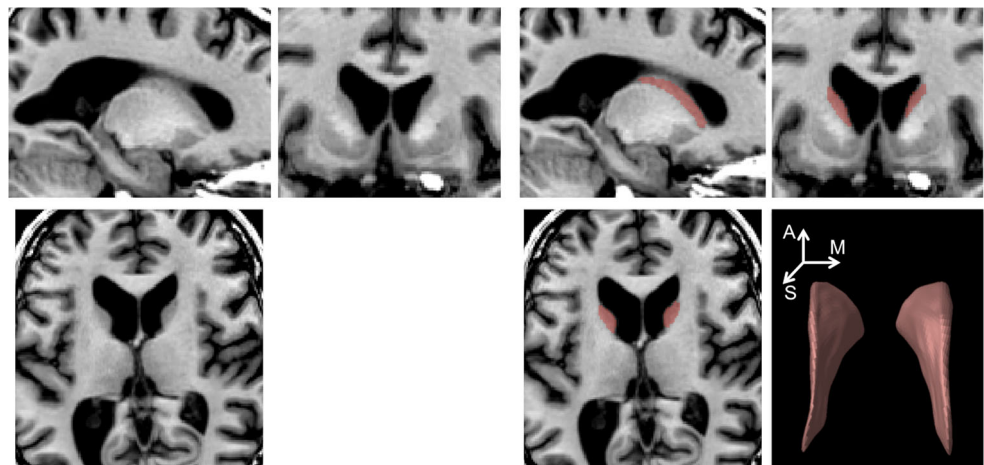
Using the 3D T1-weighted image data registered to standard stereotaxic space, boundaries of the caudate volume were manually delineated (Fig. 1) by a radiologist J.H.K. using a previously published protocol (Looi et al. 2008). The radiologist was blinded as our patients and controls were anonymized and the MRI data were randomized. The caudate was outlined by drawing lines along the medial border of the internal capsule or corona radiata and along the lateral wall of the lateral ventricle. The lower margin of the head of caudate differentiating from nucleus accumbens was outlined at the most inferior slice, in which the white matter of the internal capsule separated the caudate head clearly from the putamen. The upper margin of the caudate was defined in the most superior slice in which the caudate could be seen distinct from the wall of the lateral ventricle. The tail of caudate that curved ventrally to border the lateral atrium of the lateral ventricles was not included for analysis because of difficult

identification. Tracings were cross-referenced to both coronal and sagittal planes. In a week, the primary rater and another rater (H.K.) separately segmented 12 cases that were randomly selected. For these cases, we computed the Kappa statistic between the 1st and 2nd labeling of the primary rater, resulting in excellent agreement (intra-rater agreement: $\kappa = 90 \pm 1\%$). Comparing between the two raters, we also found excellent inter-rater reproducibility ($\kappa = 88 \pm 2\%$).

Surface-based mapping of caudate volume changes

As labels were created in a stereotaxic space, correction for intracranial volume was not required. A previously validated surface-based approach (Kim et al. 2008) was used to measure local volume changes by computing Jacobian determinants on surface-based displacement vectors between a given subject and a template surface (Styner et al. 2006). Caudate labels were converted to surface meshes using a spherical parameterization (SPHARM) based on area-preserving, distortion-minimizing mapping. Using a uniform icosahedron-subdivision of the SPHARM, we obtained a point distribution model (PDM) to allow shape-inherent point correspondences across subjects (1002 vertices). Each individual SPHARM-PDM surface was rigidly aligned to a template constructed from the mean surface of all subjects with respect to the centroid and longitudinal axes of the 1st order ellipsoid (Gerig et al. 2001). Vertex-wise displacement vectors were calculated between each individual and the overall template (Styner et al. 2006). Displacement vectors were diffused within the volume enclosed by the surface using a heat equation, yielding a displacement vector field. To assess local volume changes, we calculated Jacobian determinants from these vector fields (Kim et al. 2008). Jacobian determinants were projected back onto the template surface using tri-linear interpolation and subtracting 1, we obtained a metric of growth ($J > 0$) or shrinkage ($J < 0$) in a unit-size cube (i.e., voxel) defined on each vertex.

Fig. 1 Caudate nucleus on anatomical MRI. An expert manually delineated caudate volume (red). The 3D rendering of a labeled caudate volume is also shown (right-bottom; A: anterior, M: medial; S: superior)



Statistical analysis

Analysis was performed using SurfStat (<http://www.math.mcgill.ca/keith/surfstat/>) (Worsley et al. 2009). We used linear models for the following analyses. To identify regional volume alterations in pmHD, we compared Jacobian determinants between controls and pmHD patients using a linear model for which we performed point-wise t-tests while correcting for age and gender. We further assessed association between volume and neurocognitive scores (i.e., executive function and working memory evaluated by the NIH EXAMINER) by performing this correlation analysis while correcting for the covariate effect of the group using a linear model in order to remove a possible bias due to the skewness by group differences. We also correlated volume and disease burden (i.e., CAPs – scores based on CAG repeats and age) by Pearson's correlation coefficient. Multiple comparisons were adjusted using the false discovery rate.

Results

Group comparison

Group analysis of mean volume over all surface-points revealed bilateral global caudate volume decrease in the pmHD group compared to controls ($t = 3.4$; $FDR = 0.005$). The effect size of atrophy in the pmHD was large (Cohen's $D = 1.3$; the percent of nonoverlap between groups = 52 %). Point-wise analysis of local volumes mapped caudate atrophy in pmHD primarily onto medial surface ($t > 2.9$; $FDR < 0.05$), with most pronounced changes in anteromedial subdivision (Fig. 2; $t = 4.5$, $FDR < 0.001$ at the peak) and dorsolateral rim at the head of the caudate ($t = 7.0$, $FDR < 0.001$ at the peak). These areas showed even larger effect sizes of atrophy in the pmHD group (anteromedial subdivision: Cohen's $D = 1.8$, the nonoverlap between groups = 77.4 %; dorsolateral rim: Cohen's $D = 2.7$, nonoverlap = 82.3 %). Point-wise paired tests revealed no asymmetric atrophy in pmHD ($FDR > 0.3$).

Association with neurocognitive performance and genetic disease burden

In a combined group of patients and controls, global caudate volume positively correlated with scores of global executive function ($r = 0.6$, $FDR < 0.05$) but not with working memory ($r = 0.4$; $FDR = 0.1$). Volume within the area presenting significant group difference showed slightly higher correlations with scores of global executive function ($r = 0.8$, $FDR = 0.001$) and working memory ($r = 0.5$; $FDR < 0.05$; Fig. 3). In a separate analysis where we performed the same correlation analysis within the pmHD group, however, we found only a trend of correlation for the executive function ($r = 0.6$, $p < 0.01$ uncorrected) and no significant correlation for the working memory ($r = 0.4$, $p > 0.2$ uncorrected). This was partly due to the small sample size as the effect size of correlation coefficients was high. Point-wise analyses of local volume localized significant correlations mainly in the anteromedial subdivision.

In patients, global caudate volume did not correlate significantly with disease burden ($r = -0.4$, $FDR = 0.2$). Caudate volume within the area presenting significant group difference, however, was negatively correlated with disease burden ($r = -0.7$; $FDR = 0.01$; Fig. 4). Splitting our pmHD patients into a low-burden group ($n = 7$) and a high-burden group ($n = 7$) and testing their difference in volume, we found a significant difference ($t = 3.2$; $FDR < 0.01$).

Discussion

The current study revealed global volume loss of the caudate in subjects with premanifest Huntington's disease (pmHD), and furthermore attributed this change mainly to medial paraventricular atrophy. The caudate regional damage uncovered using our surface-based morphometry approach was concordant with the result of the previous landmark pathology study (Vonsattel et al. 1985a). This study reported that earliest changes of HD were seen in the medial paraventricular portion

Fig. 2 Group comparison of mean caudate volume (a) and local volumes (b) between patients with pmHD and controls. Caudate atrophy was found in the pmHD group and mapped on the medial surface with the most pronounced change in the region of anteromedial subregion. Gray: non-significant / colors: significant after FDR adjustment for multiple comparisons

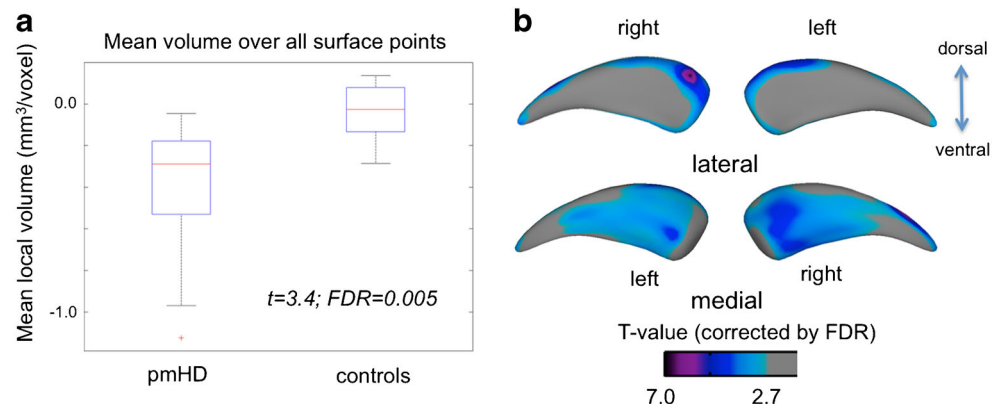
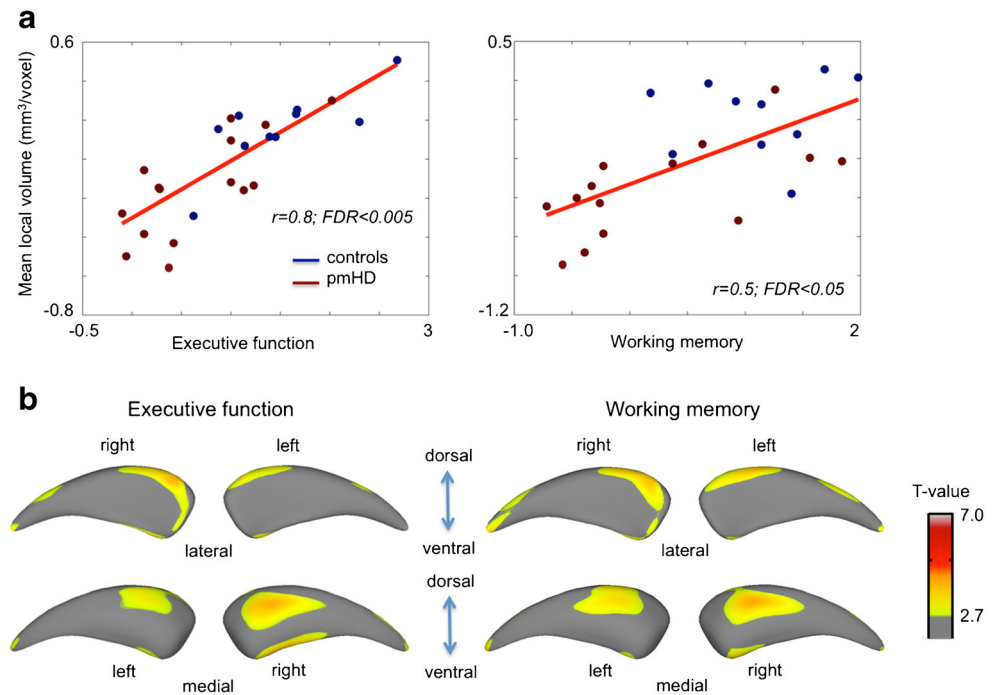


Fig. 3 Association between caudate volume and neurocognitive function. **a.** Within the area showing the significance in the group comparison, we correlated averaged volume and neurocognitive scores. We performed this correlation analysis while correcting for the covariate effect of the group using a linear model in order to remove a possible bias due to the skewness by group differences. Significant correlation was found for both executive function and working memory. **b.** Point-wise correlation analysis found the significance primarily mapped on the anteromedial subregion (FDR < 0.05)



of the caudate nucleus, tail of the caudate nucleus, and dorsal part of the putamen (Table 1).

Volumetric and surface-based shape analyses on anatomical MRI have previously attempted to replicate in vivo the regional changes observed in neuropathological studies (van den Bogaard et al. 2011; Vonsattel et al. 1985a; Younes et al. 2014). In contradistinction to our study, these studies have not consistently demonstrated subnuclear abnormalities in the caudate nucleus of subjects with pmHD. In the shape analysis by van den Bogaard et al., although they found inward displacement in the medial portion of caudate body in manifest HD, no regional significant changes were found in pmHD (van den Bogaard et al. 2011). Likewise, a more recent caudate shape analysis in pmHD (Younes et al. 2014) only found

spared dorsolateral and dorsomedial volume, and failed to reveal the caudate subnuclear atrophy that was depicted in the study of Vonsattel et al. (Vonsattel et al. 1985a). There are a few reasons why the current study was sensitive to these changes in the premanifest patients. Unlike these previous studies (van den Bogaard et al. 2011; Younes et al. 2014) that relied on single-template based automated segmentation, we manually delineated the caudate volume. We then adopted a well-established image processing method that measured Jacobian determinants derived from the point-wise displacement of the caudate surface that revealed the presence of medial paraventricular caudate atrophy in pmHD. In our previous studies (Kim et al. 2013b), we demonstrated that the popularly used displacement metric (van den Bogaard et al. 2011;

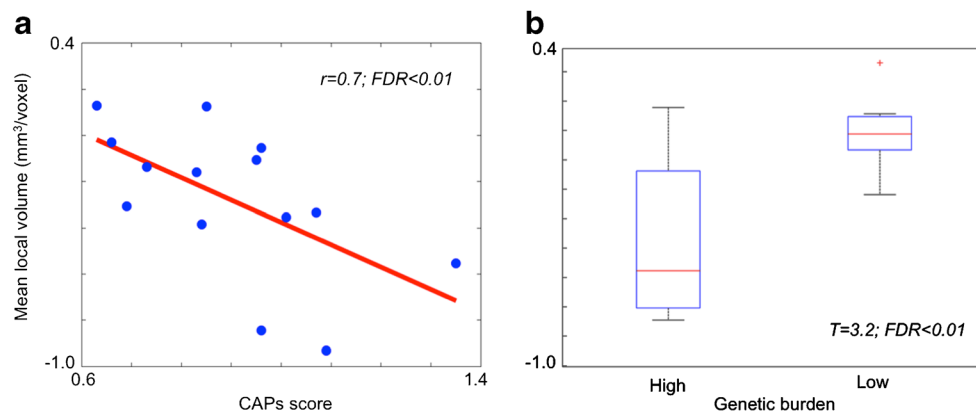


Fig. 4 Association between caudate volume and genetic disease burden. **a** Within the area showing the significance in the group comparison (Fig. 2), we correlated averaged volume and CAPs. Larger disease burden was significantly associated with smaller caudate volume

($r = 0.7$; $FDR < 0.01$). **b** We split our pmHD patients into a low-burden group ($n = 7$) and a high-burden group ($n = 7$) and tested their difference in volume: We found a significant difference ($t = 3.2$; $FDR < 0.01$)

Table 1 Demographic and examiner scores of pmHD and Controls, and CAG repeats and disease burden in pmHD

	N	Age (years)	Gender	Education (years)	Executive function	Working memory	CAG	CAPs
NC	13	45.7 (15.3)	46 % male	17.2 (1.4)	1.48 (.55)	1.08 (.51)		
pmHD	14	46.2 (11.9)	43 % male	15.7 (2.5)	.70 (.63)*	.25 (.87)*	42.4 (2.2)	.90 (.20)

Scores represent mean (standard deviation)

* Significantly lower in pmHD group than NC ($p < 0.05$ after Bonferroni adjustment)

Younes et al. 2014) could be entangled with various morphological changes including volume, local shift and bending. Differentiating volume changes from other morphological characteristics may also explain the superior sensitivity in the current study.

Our previous study using 7 T MRI found that a positive phase shift (attributed to elevated iron concentration) in the caudate correlated negatively with genetic disease burden and neurocognitive assessments of executive function and working memory of the NIH EXAMINER (Apple et al. 2014), suggesting that the magnitude of microstructural changes in pmHD reflects the severity of neurocognitive deficits. Similarly, our morphometry study showed that caudate regional volume also correlated with genetic and neurocognitive scores of pmHD. Taken together, these studies highlight that both microstructural and macrostructural changes in the caudate can be observed in pmHD and that these changes are associated with executive dysfunction and time to manifest HD.

Previous studies have proposed a slightly different topographical organization of the caudate (Kim et al. 2013a; Nakano 2000; Parent and Hazrati 1995; Postuma and Dagher 2006; Selemon and Goldman-Rakic 1988). A rough demarcation with 3 defined functional zones is however largely accepted: associative striatum (head of caudate), sensorimotor striatum (dorsolateral rim of the caudate), and the limbic striatum (ventral caudate). Our finding of caudate atrophy in relation to preHD was mapped mainly on anteromedial sub-region that corresponded to the head of caudate. A recent meta-analysis of functional MRI has shown that the head of the caudate nucleus is activated mainly in relation to cognitive and emotional processes (Robinson et al. 2012). This study further showed that the head of the caudate had functional connectivity with the amygdala and portions of the anterior and posterior cingulate (BA32 and 31, respectively) that are involved in emotive and cognitive process whereas the posterior portion of the caudate displayed functional connectivity with regions involved in motor control (superior and medial frontal cortices including BA6 and BA8), and perception related processes (clusters in occipital lobe, the parietal lobe, and the posterior cingulate). This is also confirmed by a thorough review on functional and structural connectivity of cognition and emotion (Pessoa 2008). It remains to be

investigated whether the neocortical cortices that are functionally and structurally linked with the primary site of caudate damage in pmHD are also affected.

Our study has several limitations. First, the number of subjects was small; however, most of our findings were significant after correction for multiple comparisons. It is also noted that the expert had a degree of difficulty in finding landmarks for labeling the caudate volume depending on the area. Nevertheless, such difficulty did not influence much the overall reproducibility of the manual labeling as we found a high intra-rater agreement using the kappa statistics. Regionally, the biggest uncertainty in identification of the landmark occurred at the level of the tail, which has been common in many previous articles as commented in literature (Looi et al. 2008). This may be the main reason why we did not observe the known dorsal-to-ventral gradients of HD progression (Vonsattel 2008) although our study revealed the medial-to-lateral gradient of caudate. Finally, the present study examined only the caudate nucleus by performing a cross-sectional analysis. To generalize and complement the outcome of the present study, future work should include other striatal and extrastriatal structures and multiple time points of each patient using a longitudinal design. This may assess the spatiotemporal disease progression more precisely and the viability of these imaging markers as outcomes in clinical trials.

In conclusion, analyzing patients with pmHD, our surface-based morphometric technique revealed an early sign of caudate subnuclear structural damages, which was associated with disease burden. The association with other clinical profiles such as scores in executive function, and working memory may need a further clarification with a larger sample study. Elucidating caudate atrophy using the employed subregional volumetry techniques has the potential to provide a more powerful biomarker than total caudate volumes because we could identify the regions most atrophied at this early stage and demonstrate relationships to key clinical variables.

Compliance with ethical standards This study was supported by University of California Discovery ITL-BIO04–10148, an academic-industry partnership grant with GE Healthcare, the National Institutes of Health grant 1S10RR026845–01, and National Institute on Aging (NIA) grant K23AG037566.

H.K. is supported by the Banting Postdoctoral Fellowships and Fonds de recherche Santé Québec (FRSQ) Postdoctoral Training Award.

K.P. is supported by the NIA K23AG037566, the Hellman Family Foundation, Quest Diagnostics.

Conflict of interest All authors report no biomedical financial interests or potential conflicts of interest.

Ethical approval All procedures performed in studies involving human participants were in accordance with the ethical standards of our institutional and/or national research committee and with the 1964 Helsinki declaration and its later amendments or comparable ethical standards.

Informed consent Informed consent was obtained from all individual participants included in the study.

References

- Apple, A. C., Possin, K. L., Satriis, G., Johnson, E., Lupo, J. M., Jakary, A., Wong, K., Kelley, D. A., Kang, G. A., Sha, S. J., Kramer, J. H., Geschwind, M. D., Nelson, S. J., & Hess, C. P. (2014). Quantitative 7 T phase imaging in premanifest Huntington disease. *AJNR. American Journal of Neuroradiology*, *35*, 1707–1713.
- Aylward, E. H., Codori, A. M., Barta, P. E., Pearlson, G. D., Harris, G. J., & Brandt, J. (1996). Basal ganglia volume and proximity to onset in presymptomatic Huntington disease. *Archives of Neurology*, *53*, 1293–1296.
- Aylward, E. H., Liu, D., Nopoulos, P. C., Ross, C. A., Pierson, R. K., Mills, J. A., Long, J. D., Paulsen, J. S., Investigators, P.-H., & Coordinators of the Huntington Study, G (2012). Striatal volume contributes to the prediction of onset of Huntington disease in incident cases. *Biol Psychiatry*, *71*, 822–828.
- Cheng, Y., Peng, Q., Hou, Z., Aggarwal, M., Zhang, J., Mori, S., Ross, C. A., & Duan, W. (2011). Structural MRI detects progressive regional brain atrophy and neuroprotective effects in N171-82Q Huntington's disease mouse model. *Neuroimage*, *56*, 1027–1034.
- Dogan, I., Eickhoff, S. B., Schulz, J. B., Shah, N. J., Laird, A. R., Fox, P. T., & Reetz, K. (2013). Consistent neurodegeneration and its association with clinical progression in Huntington's disease: a coordinate-based meta-analysis. *Neuro-Degenerative Diseases*, *12*, 23–35.
- Dominguez, D.J., Stout, J.C., Poudel, G., Churchyard, A., Chua, P., Egan, G.F., Georgiou-Karistianis, N., (2015). Multimodal imaging biomarkers in premanifest and early Huntington's disease: 30-month IMAGE-HD data. *Br J Psychiatry*.
- Duff, K., Paulsen, J. S., Beglinger, L. J., Langbehn, D. R., Stout, J. C. & Predict-HD Investigators. (2007). Psychiatric symptoms in Huntington's disease before diagnosis: the predict-HD study. *Biology Psychiatry*, *62*(12), 1341–1346.
- Duff, K., Paulsen, J. S., Beglinger, L. J., Langbehn, D. R., Wang, C. C., Stout, J. C., Ross, C. A., Aylward, E., Carlozzi, N. E., Queller, S., & Grp, H. S. (2010). Frontal" behaviors before the diagnosis of Huntington's disease and their relationship to markers of disease progression: evidence of early lack of awareness. *Journal of Neuropsychiatry and Clinical Neurosciences*, *22*, 196–207.
- Finkbeiner, S. (2010). Bridging the valley of death of therapeutics for neurodegeneration. *Nature Medicine*, *16*, 1227–1232.
- Fonov, V., Evans, A. C., Botteron, K., Almli, C. R., McKinstry, R. C., Collins, D. L., & Brain Development Cooperative, G. (2011). Unbiased average age-appropriate atlases for pediatric studies. *Neuroimage*, *54*, 313–327.
- Gerig, G., Styner, M., Jones, D., Weinberg, D. R., & Lieberman, J. (2001). Shape analysis of brain ventricles using SPHARM. *MMBIA*, 171–178.
- Gusella, J. F., McNeil, S., Persichetti, F., Srinidhi, J., Novelletto, A., Bird, E., Faber, P., Vonsattel, J. P., Myers, R. H., & MacDonald, M. E. (1996). Huntington's disease. *Cold Spring Harbor Symposia on Quantitative Biology*, *61*, 615–626.
- Hart, E., Middelkoop, H., Jurgens, C. K., Witjes-Ane, M. N., & Roos, R. A. (2011). Seven-year clinical follow-up of premanifest carriers of Huntington's disease. *PLoS Curr*, *3*, RRN1288.
- Holl, A. K., Wilkinson, L., Tabrizi, S. J., Painold, A., & Jahanshahi, M. (2013). Selective executive dysfunction but intact risky decision-making in early Huntington's disease. *Movement Disorders*, *28*, 1104–1109.
- Joo, E. Y., Kim, H., Suh, S., & Hong, S. B. (2014). Hippocampal substructural vulnerability to sleep disturbance and cognitive impairment in patients with chronic primary insomnia: magnetic resonance imaging morphometry. *Sleep*, *37*, 1189–1198.
- Kim, H., Besson, P., Colliot, O., Bernasconi, A., & Bernasconi, N. (2008). Surface-based vector analysis using heat equation interpolation: a new approach to quantify local hippocampal volume changes. *Med Image Comput Comput Assist Interv*, *5241*, 1008–1015.
- Kim, D. J., Park, B., & Park, H. J. (2013a). Functional connectivity-based identification of subdivisions of the basal ganglia and thalamus using multilevel independent component analysis of resting state fMRI. *Human Brain Mapping*, *34*, 1371–1385.
- Kim, H., Mansi, T., & Bernasconi, N. (2013b). Disentangling hippocampal shape anomalies in epilepsy. *Frontiers in Neurology*, *4*.
- Kramer, J. H., Mungas, D., Possin, K. L., Rankin, K. P., Boxer, A. L., Rosen, H. J., Bostrom, A., Sinha, L., Berhel, A., & Widmeyer, M. (2014). NIH EXAMINER: conceptualization and development of an executive function battery. *Journal of the International Neuropsychological Society*, *20*, 11–19.
- Looi, J. C., Lindberg, O., Liberg, B., Tatham, V., Kumar, R., Maller, J., Millard, E., Sachdev, P., Hogberg, G., Pagani, M., Botes, L., Engman, E. L., Zhang, Y., Svensson, L., & Wahlund, L. O. (2008). Volumetrics of the caudate nucleus: reliability and validity of a new manual tracing protocol. *Psychiatry Research*, *163*, 279–288.
- Nakano, K. (2000). Neural circuits and topographic organization of the basal ganglia and related regions. *Brain Dev*, *22*(Suppl 1), S5–16.
- Parent, A., & Hazrati, L. N. (1995). Functional anatomy of the basal ganglia. I. The cortico-basal ganglia-thalamo-cortical loop. *Brain Research. Brain Research Reviews*, *20*, 91–127.
- Paulsen, J. S., Hayden, M., Stout, J. C., Langbehn, D. R., Aylward, E., Ross, C. A., Guttman, M., Nance, M., Kiebertz, K., Oakes, D., Shoulson, I., Kayson, E., Johnson, S., Penziner, E., & Investigators, P.-H. (2006). Preparing for preventive clinical trials - the predict-HD study. *Archives of Neurology*, *63*, 883–890.
- Paulsen, J. S., Langbehn, D. R., Stout, J. C., Aylward, E., Ross, C. A., Nance, M., Guttman, M., Johnson, S., MacDonald, M., Beglinger, L. J., Duff, K., Kayson, E., Biglan, K., Shoulson, I., Oakes, D., Hayden, M., & Coordin, P. H. I. (2008). Detection of Huntington's disease decades before diagnosis: the predict-HD study. *Journal of Neurology Neurosurgery and Psychiatry*, *79*, 874–880.
- Pessoa, L. (2008). On the relationship between emotion and cognition. *Nature Reviews Neuroscience*, *9*, 148–158.
- Postuma, R. B., & Dagher, A. (2006). Basal ganglia functional connectivity based on a meta-analysis of 126 positron emission tomography and functional magnetic resonance imaging publications. *Cerebral Cortex*, *16*, 1508–1521.
- Read, J., Jones, R., Owen, G., Leavitt, B. R., Coleman, A., Roos, R. A., Dumas, E. M., Durr, A., Justo, D., Say, M., Stout, J. C., Tabrizi, S. J., Craufurd, D., & Investigators, T.-H. (2013). Quality of life in Huntington's disease: a comparative study investigating the impact

- for those with pre-manifest and early manifest disease, and their partners. *J Huntingtons Dis*, 2, 159–175.
- Robinson, J. L., Laird, A. R., Glahn, D. C., Blangero, J., Sanghera, M. K., Pessoa, L., Fox, P. M., Uecker, A., Friehs, G., Young, K. A., Griffin, J. L., Lovallo, W. R., & Fox, P. T. (2012). The functional connectivity of the human caudate: an application of meta-analytic connectivity modeling with behavioral filtering. *Neuroimage*, 60, 117–129.
- Roos, R. A., Pruyt, J. F., de Vries, J., & Bots, G. T. (1985). Neuronal distribution in the putamen in Huntington's disease. *Journal of Neurology, Neurosurgery, and Psychiatry*, 48, 422–425.
- Selemon, L. D., & Goldman-Rakic, P. S. (1988). Common cortical and subcortical targets of the dorsolateral prefrontal and posterior parietal cortices in the rhesus monkey: evidence for a distributed neural network subserving spatially guided behavior. *The Journal of Neuroscience*, 8, 4049–4068.
- Sled, J. G., Zijdenbos, A. P., & Evans, A. C. (1998). A nonparametric method for automatic correction of intensity nonuniformity in MRI data. *IEEE Transactions on Medical Imaging*, 17, 87–97.
- Stout, J. C., Paulsen, J. S., Queller, S., Solomon, A. C., Whitlock, K. B., Campbell, J. C., Carlozzi, N., Duff, K., Beglinger, L. J., Langbehn, D. R., Johnson, S. A., Biglan, K. M., & Aylward, E. H. (2011). Neurocognitive signs in prodromal Huntington disease. *Neuropsychology*, 25, 1–14.
- Styner, M., Oguz, I., Xu, S., Brechb'uhler, C., Pantazis, D., Gerig, G., 2006. Statistical Shape Analysis of Brain Structures using SPHARM-PDM. MICCAI 2006 OpenSource workshop.
- van den Bogaard, S. J., Dumas, E. M., Ferrarini, L., Milles, J., van Buchem, M. A., van der Grond, J., & Roos, R. A. (2011). Shape analysis of subcortical nuclei in Huntington's disease, global versus local atrophy—results from the TRACK-HD study. *Journal of the Neurological Sciences*, 307, 60–68.
- Vonsattel, J. P. G. (2008). Huntington disease models and human neuropathology: similarities and differences. *Acta Neuropathologica*, 115, 55–69.
- Vonsattel, J. P., Myers, R. H., Stevens, T. J., Ferrante, R. J., Bird, E. D., & Richardson, E. P. (1985a). Neuropathological classification of Huntingtons-disease. *Journal of Neuropathology and Experimental Neurology*, 44, 559–577.
- Weir, D. W., Sturrock, A., & Leavitt, B. R. (2011). Development of biomarkers for Huntington's disease. *Lancet Neurology*, 10, 573–590.
- Worsley, K., Taylor, J. E., Carbonell, F., Chung, M. K., Duerden, E. G., Bernhardt, B., Lyttelton, O., Boucher, M., & Evans, A. C. (2009). SurfStat: A Matlab toolbox for the statistical analysis of univariate and multivariate surface and volumetric data using linear mixed effects models and random field theory. *Neuroimage*, 47, 451 SA-AM.
- You, S. C., Satris, G., Apple, A., Frazier, D., Sha, S., Hess, C., Geschwind, M., Kramer, J., & Possin, K. (2013). New sensitive measures of executive functioning in premotor Huntington's disease. *Neurology*, 80.
- You, S. C., Geschwind, M. D., Sha, S. J., Apple, A., Satris, G., Wood, K. A., Johnson, E. T., Gooblar, J., Feuerstein, J. S., Finkbeiner, S., Kang, G. A., Miller, B. L., Hess, C. P., Kramer, J. H., & Possin, K. L. (2014). Executive functions in premanifest Huntington's disease. *Movement Disorders*, 29, 405–409.
- Younes, L., Ratnanather, J. T., Brown, T., Aylward, E., Nopoulos, P., Johnson, H., Magnotta, V. A., Paulsen, J. S., Margolis, R. L., Albin, R. L., Miller, M. I., Ross, C. A., & Coordinat, P.-D. I. (2014). Regionally selective atrophy of subcortical structures in prodromal HD as revealed by statistical shape analysis. *Human Brain Mapping*, 35, 792–809.
- Zhang, Y., Long, J. D., Mills, J. A., Warner, J. H., Lu, W. J., & Paulsen, J. S. (2011). Indexing disease progression at study entry with individuals At-risk for Huntington disease. *American journal of medical genetics part B-neuropsychiatric. Genetics*, 156b, 751–763.